

# Effect of back electrode on photovoltaic properties of crystal-violet-dye-doped solid-state thin film

Ajanta Haldar · Subhasis Maity · N. B. Manik

Received: 8 September 2007 / Revised: 18 November 2007 / Accepted: 4 December 2007 / Published online: 13 February 2008  
© Springer-Verlag 2007

**Abstract** Recently, organic/polymeric materials are being widely used to develop photovoltaic devices. In our earlier work, we have studied the photovoltaic property of crystal violet in solid-state photoelectrochemical cell (PEC), but the power conversion efficiency is quite low. In this work, we have used aluminium-coated mylar as a back electrode to enhance the power conversion efficiency. Because of the insertion of a reflecting back electrode, the charge carriers are confined in the active layer which enhances the efficiency from 0.144% to 0.670%. Thin film polymer PEC has been prepared by using optically active crystal violet dye. The dye was dispersed in polyvinyl alcohol used as an inert polymer binder and polyethylene oxide complexed with lithium perchlorate ( $\text{LiClO}_4$ ) ion salt as a solid electrolyte with ethylene carbonate and propylene carbonate as plasticisers. With this blend, two cells have been prepared. In one cell, this blend is sandwiched between indium-tin-oxide-coated glass plate and aluminium plate whereas the modification of the cell is done using highly polished aluminium-coated mylar sheet in place of Al electrode. Dark  $I$ - $V$  characteristics are measured and compared for these cells. Improvement of photovoltaic parameters has been observed in the case of polished mylar electrode.

**Keywords** Photoelectrochemical cell · Conversion efficiency · Back electrode · Crystal violet · Thin film

## Introduction

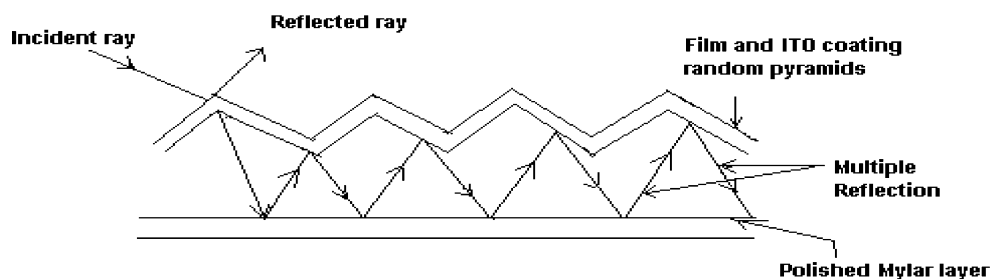
Organic/polymer materials have opened a new dimension in the field of material science. Recently, attempts are being made to develop photovoltaic devices/solar cells by using different organic/polymer materials. Large area photovoltaic devices can be prepared by easy-processing techniques such as spin coating, dip coating, sol gel technique, etc. At present, the quantum efficiency of organic photovoltaic devices is low. But it is increasing gradually by using different preparation techniques and selection of different materials, electrodes, device architectures, etc. Generally, in photovoltaic device [1–10] applications, a thin layer of organic materials is sandwiched between two electrodes. Light is being incident from the front electrode which is a transparent conducting glass plate having high work function. Materials having low work function are used as back electrodes [11–14]. Generally, indium tin oxide (ITO)-coated glass plate is used as a conducting glass plate. The performance of the devices significantly depends on the back electrodes also. The study on the effect of back electrodes is useful to understand the device mechanism.

In our earlier works [15–19], we have also reported that the solid-state dye-doped PEC can be used for light detection. But there is no such report on photovoltaic devices based on this principle.

The PEC under study contains a blend made of crystal violet dye dispersed in transparent polyvinyl alcohol (PVA), polyethylene oxide (PEO) complexed with lithium perchlorate ( $\text{LiClO}_4$ ), ethylene carbonate (EC) and propylene carbonate (PC). Crystal violet dye is used as an optical active material and is dispersed in PVA, which acts as an inert binder.  $\text{LiClO}_4$  is mixed with solid polymer matrix PEO to form the solid-state ionic conductor. The ionic conductivity of PEO to  $\text{LiClO}_4$  complexes is very low [20–21]. The use of a plasticiser is a common technique to enhance the ionic

A. Haldar (✉) · S. Maity · N. B. Manik  
Condensed Matter Physics Research Centre,  
Department of Physics, Jadavpur University,  
Kolkata 700032 West Bengal, India  
e-mail: ahaldar\_ju2003@yahoo.com

**Fig. 1** Principle of operation of multiple reflection



conductivity [7]. In this system, we have used EC dissolved in PC as plasticisers to enhance the mobility of the charge carriers. One solid film of this blend is sandwiched between transparent indium tin oxide (ITO)-coated glass plate and Al plate, which acts as two contact electrodes.

Another solid film of this blend is sandwiched between transparent indium tin oxide (ITO)-coated glass plate and mylar sheet. Here, aluminium-coated mylar surface is used as reflected back surface electrode which is used to compare the photovoltaic parameters from the previously prepared cell.

Light entering the stack of layers will be absorbed in all layers of the cell. In the intrinsic layer (active layer), the absorbed light forms an electron–hole pair. Because of internal electric field in intrinsic layer, the electrons and holes are separated and collected by front and back contacts. Thus, the incident optical energy is confined within two electrodes, which is enhanced because of multiple reflection in the presence of polished mylar layer. The principle of the operation is shown in Fig. 1.

In this work, dark  $I$ – $V$  characteristics and the photovoltaic currents with different intensities have been measured for the purpose of comparison. Improvement of photovoltaic parameters [1–2] such as open circuit voltage  $V_{oc}$ , short circuit current  $I_{sc}$ , fill factor FF and conversion efficiency  $\eta$  has been observed while indium tin oxide (ITO)-coated glass plate and polished Al-coated mylar electrode are used as two counter electrodes. Enhancement of photovoltaic parameters in the case of reflecting back surface cell reveals that the total incident optical energy is confined within two electrodes because of multiple reflection [13, 14].

## Experimental

### Sample preparation

Crystal violet dye (BDH, England, UK) was recrystallised twice from ethanol–water mixture and mixed with PVA (S. D. Fine Chem. Ltd., Boisar, India; M.W. 125,000) used as a transparent inert binder. In a clean test tube, 5 g of PVA was mixed with 10 cc of double distilled water, warmed gently and stirred to make a transparent viscous solution of PVA. Two milligrams of crystal violet (cationic dye) is mixed with this solution. Absorption peak of crystal violet dye is at 590 nm in water solution.

The quantum yield of this dye is quite high. PVA was used here as an inert transparent binder to form the stable film of the dye.

In a separate beaker cleaned by regular processes, a solid electrolyte was prepared by mixing PEO (BDH, England, UK; M.W. 600,000),  $\text{LiClO}_4$  (Fluka, 99.5% pure), EC (Fluka, 99.5% pure) and PC (Fluka, 99.5% pure). The complex of PEO,  $\text{LiClO}_4$ , EC, PC (30.60%, 3.60%, 19.60% and 46.20% by weight) were mixed, stirred and heated around a temperature 80 °C for 5 h. This gel-like solid electrolyte is mixed with the previously prepared dye–PVA solution to form the blend. This blend is heated at a temperature 80 °C and stirred properly to mix them well for about 1 hr.

The electrodes were cleaned in a chloroform solution and dried under vacuum about 5 h before use. With the help of a viscous gel-like solid solution, the thin film is sandwiched between transparent ITO-coated glass plate and another Al-coated mylar sheet as reflecting back surface. Spin coating unit is used to form the film of uniform thickness. Another thin film is also formed with the help of the above procedure where ITO-coated glass plate and Al plates are used as counter electrodes.

The two electrical leads are taken out from the two ends of the two electrodes of each cell. The complete cells are vacuum dried for about 12 h at around 80 °C before the final measurement. The structure of the PEC is shown in Fig. 2.

### Measurements

To measure the dark  $I$ – $V$  characteristics, two cells are biased with a dc source with a series resistance of 56 k $\Omega$ .

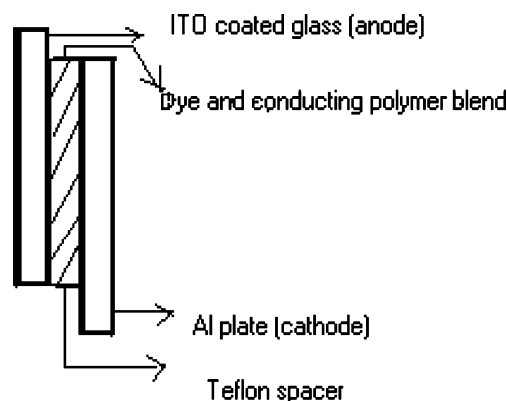


**Fig. 2** Structure of photoelectrochemical cell

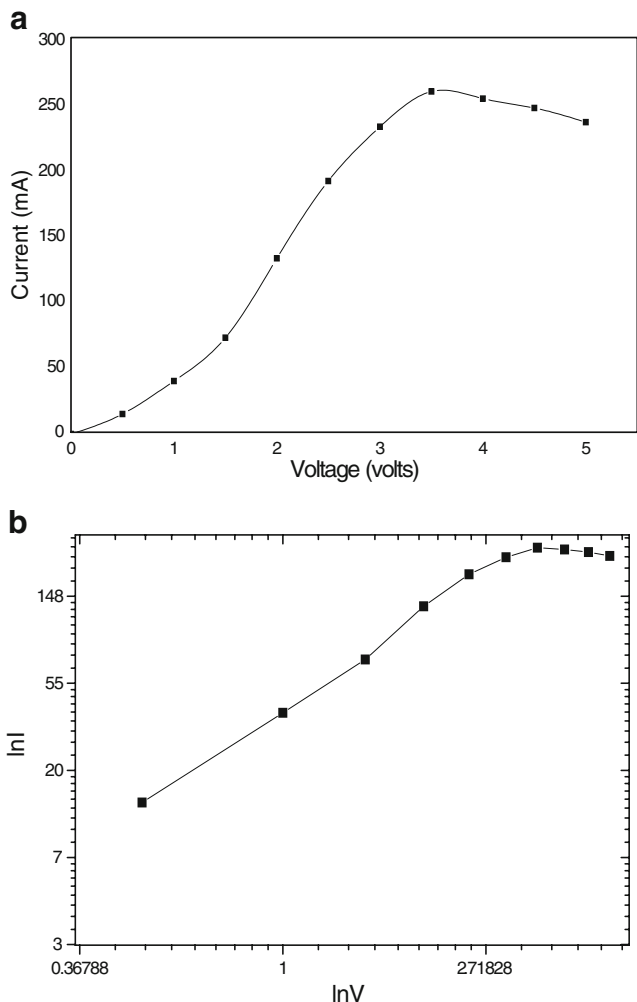


**Fig. 3** **a** Dark  $I$ - $V$  characteristic plot (with mylar). **b**  $\ln I$  vs  $\ln V$  plot (with mylar)

The current flowing through the device was estimated by measuring the voltage drop (measured by Agilent data acquisition unit, Model No: 34970A) across this sensing resistance. Dividing the measured voltage by the value of this sensing resistance, the current flowing through the device is calculated. For optical measurement, a tungsten lamp of 200 W is used. Light is allowed to strike on the cell. Varying the intensity of incident radiation voltage drop and hence the photocurrent across the sensing resistance is measured. The intensity is measured by a calibrated lux meter (Kyoritsu Electrical Instruments Works Ltd. Tokyo, model 5200). Photocurrent is measured by varying the intensity.

**Results and discussion**

**Dark  $I$ - $V$  characteristics**

As mentioned before, an ionic salt  $\text{LiClO}_4$  is used and is expected that the positive ions from  $\text{LiClO}_4$  salt are

accumulated near the cathode and the negative ions near the anode upon application of external bias on the device. A depletion layer is formed inside the active layer because of the redistribution of ionic charges in a similar manner as found in the case of light-emitting electrochemical cell [22–24] used to develop organic light-emitting diodes.

The  $I$ - $V$  curves of two films are shown in Figs. 3(a) and 4(a). Logarithmic plots of the current vs bias voltage are shown in Figs. 3(b) and 4(b). The  $\ln I$ - $\ln V$  plot shows a transition point at a bias voltage of 2.0 V, which seems to indicate a change in current conduction mechanism. As the organic materials are disordered solids, there is no well-defined band structure. The molecules are bound together with weak van der Waals forces, and the charge transport occurs through the loosely bound  $\pi$ -conjugated electrons. Here, instead of conduction and valance band, there are lowest unoccupied molecular orbital (LUMO) and highest occupied molecular orbital (HOMO) levels. This energy difference ( $E_g$ ) between the LUMO and HOMO states is equal to the electrochemical redox potential of the organic

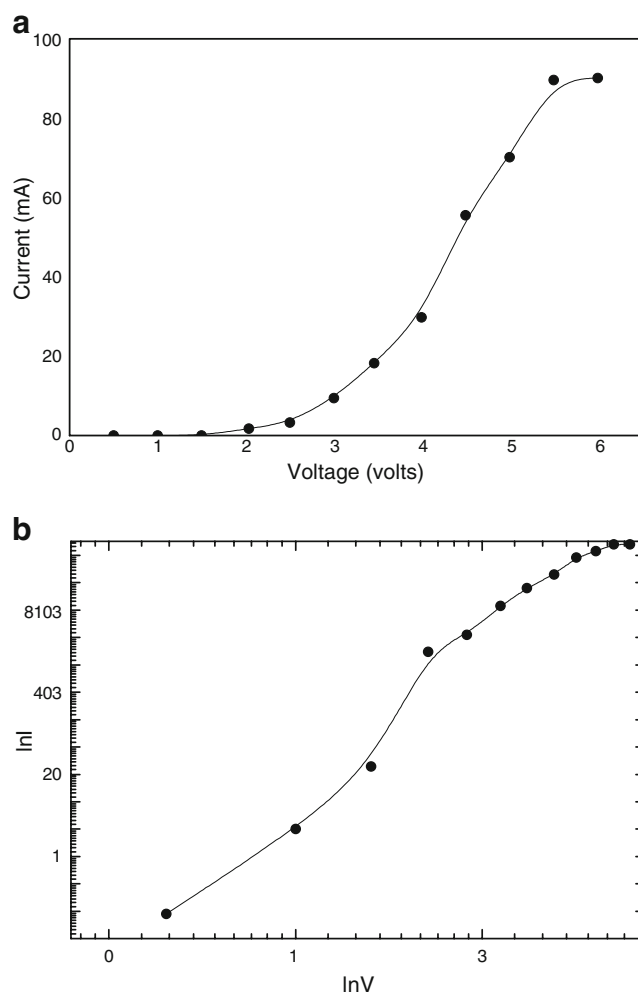


**Fig. 4** **a** Dark  $I$ - $V$  characteristic plot (without mylar). **(b)**  $\ln I$  vs  $\ln V$  plot (without mylar)

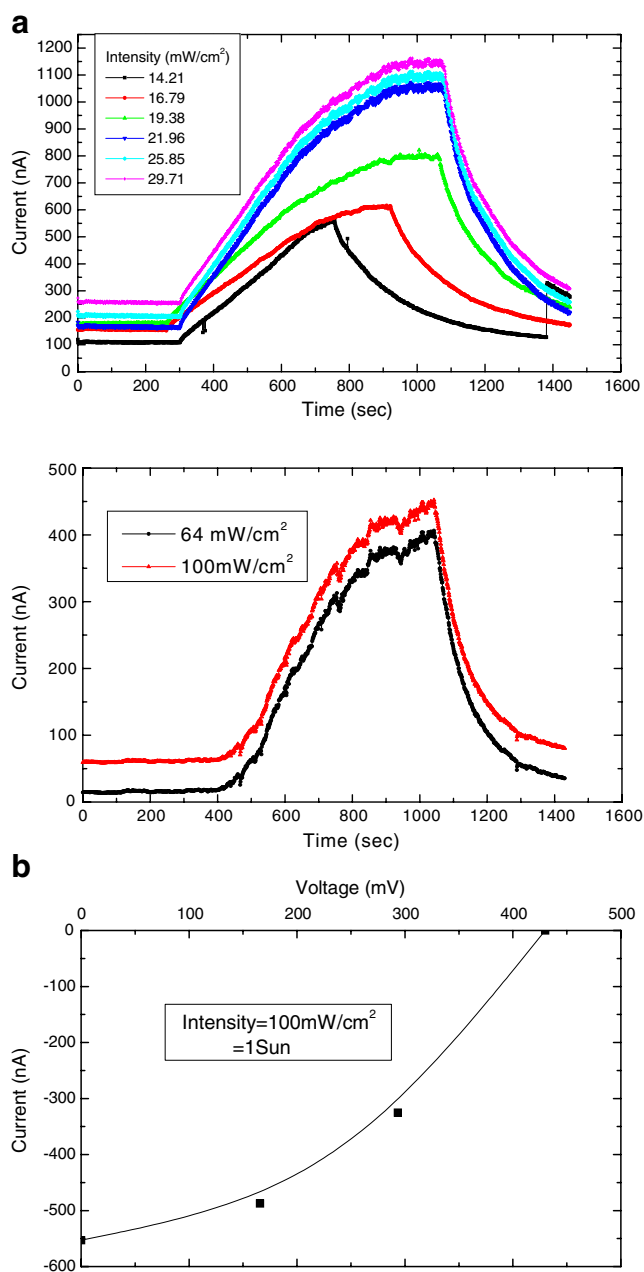


**Fig. 5** a Photocurrent at different intensities of incident illumination (with mylar). (b)  $I$ - $V$  characteristics at 1 Sun incident illumination

material. Application of bias voltage greater than the threshold voltage ( $V_{ON}$ ) will dope the material p-type and n-type simultaneously [25]. So, the voltage at which this process occurs is given by

$$E_g = eV_{ON} \tag{1}$$

where  $E_g$  is the band gap.

Here  $E_g=2.0$  eV whereas the actual value of the band gap of the dye is 2.1 eV. This deviation is quite reasonable within our experimental limit. Though the blend is a mixture of different materials, it is expected that the dye plays a major role in charge conduction mechanism.

As mentioned,  $\ln I$ - $\ln V$  relation is linear which shows a power law relation of  $I$ - $V$  of the form

$$I \propto V^{m+1} \tag{2}$$

where  $m$  is constant.

In our case,  $m$  has two values. Below transition, i.e. within the region  $V < 2$  V,  $m=1$  which indicates the conduction process is ohmic and for above transition  $V > 2$  V,  $m=4$  which indicates trap charge-assisted conduction process.

The dark  $I$ - $V$  curve can be fitted with the assumption that during conduction, carriers are trapped at different trap levels between LUMO and HOMO. To explain the charge conduction mechanism beyond the ohmic region, a model based on trap charges is considered [24, 26]. The starting equations are one-dimensional single (double) carrier drift current and Poisson equations (e. g. for electron or holes or both of them):

$$J_d = nquE \tag{(3a)}$$

$$\frac{dE}{dx} = \frac{q}{E}(n + n_t) \tag{(3b)}$$

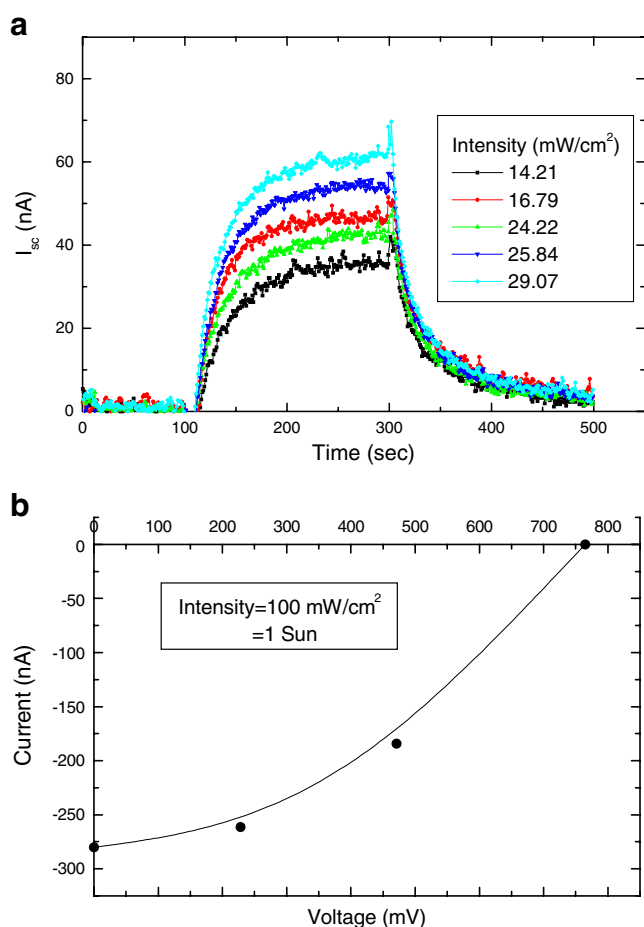


**Fig. 6** a Photocurrent at different intensities of incident illumination (without mylar). (b)  $I$ - $V$  characteristics at 1 Sun incident illumination

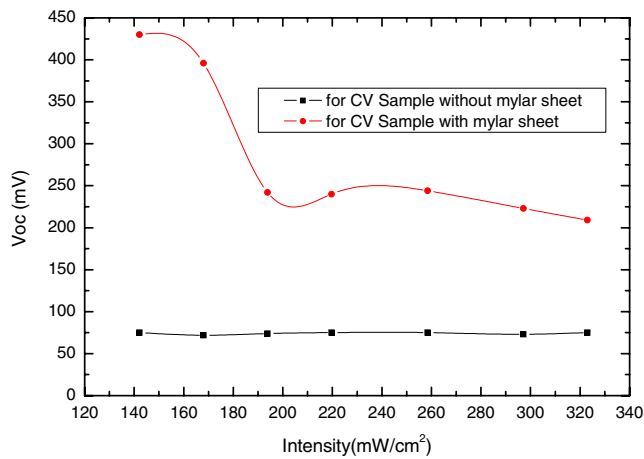


Fig. 7 Intensity vs  $V_{oc}$  curve

where  $J_d$  is the current density,  $\mu$  is the carrier mobility,  $E$  is the electric field strength,  $n$  and  $n_t$  are the free and trapped charge concentrations, respectively,  $q$  is the unit charge and  $\epsilon$  is equal to  $\epsilon_0\epsilon_r$  with  $\epsilon_0$  being the permittivity of vacuum and  $\epsilon_r$  the relative dielectric constant. When traps have an exponential energy distribution, the trap charge concentration ( $n_t$ ) is

$$n_t = H_n \exp\left(\frac{F_n}{KT_t}\right) \tag{4}$$

where  $H_n$  is the trap density,  $F_n$  is the electron fermi energy,  $K$  is Boltzmann’s constant and  $T_t$  is the characteristic temperature of the exponential trap distribution (i.e.  $T_t = E_t/K$ , where  $E_t$  is the characteristic trap energy). Solving Eqs. 3a and 3b with the above distribution of traps, the current voltage characteristic has the form

$$J = N_c\mu q^{1-m} \left(\frac{m\epsilon}{H_n(m+1)}\right)^m \left(\frac{2m+1}{m+1}\right)^{m+1} \frac{V^{m+1}}{L^{2m+1}} \tag{5}$$

$$\text{i.e. } I = A \cdot N_c\mu q^{1-m} \left(\frac{m\epsilon}{H_n(m+1)}\right)^m \left(\frac{2m+1}{m+1}\right)^{m+1} \frac{V^{m+1}}{L^{2m+1}} \tag{6}$$

where  $m = T_t/T$  and  $A$  is the effective surface area of the film. The most notable feature in the above equation is the power law dependence  $I \sim V^{m+1}$ .

To calculate this trap energy  $E_t$ , we have to calculate characteristics trap temperature  $T_t$  where  $T$  is room temperature

$$T_t = mT$$

$$T_t = 1,200K \tag{7}$$

So  $E_t = 0.103\text{eV}$ .

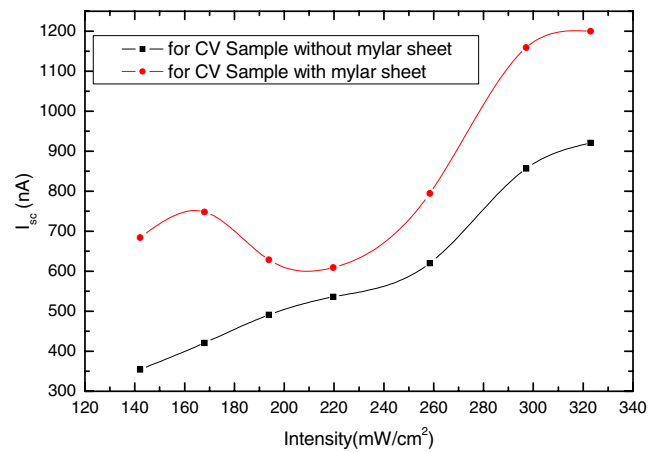


Fig. 8 Intensity vs  $I_{sc}$  curve

Photovoltaic measurements

Measurement of  $I_{sc}$  and  $V_{oc}$  is done under 1 Sun constant illumination. The variations of short circuit current ( $I_{sc}$ ) with time ( $t$ ) for different intensity illumination for two cells are shown in Figs. 5(a) and 6(a). Here, both the cells are illuminated through the ITO side.

Furthermore, experimental evidences of this effect are presented in Figs. 7 and 8 where the short circuit current ( $I_{sc}$ ) and open circuit voltage ( $V_{oc}$ ) are plotted as function of intensity of incident light.

Various photovoltaic parameters such as  $V_{oc}$  and  $I_{sc}$  are obtained to be 765 mV and 280 nA, respectively in the case of cell made up with ITO-coated glass plate and Al electrode. In the case of cell made up with ITO-coated glass plate and Al-coated mylar, the values of  $V_{oc}$  and  $I_{sc}$  are obtained to be 430 mV and 553 nA. The power conversion efficiency of each cell can be estimated by using Eqs. 1 and 2 of our previous paper [19].

The estimated values of FF and power conversion efficiency [19] are 0.33% and 0.144%, respectively for the cell without myla. Using reflecting mylar surface as back electrode, the values of FF and power conversion efficiency are enhanced up to 0.35% and 0.670%. The values of photovoltaic parameters of the two cells are shown in Table 1.

Table 1 Values of the photovoltaic parameters of the two cells

Parameters	Cell using ITO–Al as electrodes	Cell using ITO–Al-coated mylar as electrodes
Short circuit current ( $I_{sc}$ )	280 nA	553 nA
Open circuit voltage ( $V_{oc}$ )	765 mV	430 mV
Fill factor (FF)	0.33	0.35
Power conversion efficiency ( $\eta$ )	0.144%	0.670%

The increasing value of the photovoltaic parameter reveals that, because of multiple reflection from polished back electrode surface, the confinement of incident optical energy becomes larger. As the incident illumination gradually increases the number of generated photocarriers, the value of  $I_{sc}$  increases gradually. After a certain time, the photocarrier becomes saturated. In the case of using Al-coated mylar layer as counter electrode instead of Al electrode, the confinement of optical energy becomes multiplied, which causes the enhancement of photovoltaic parameters ( $I_{sc}$ ,  $\eta$ ).

The experimental results (Fig. 7) show that  $V_{oc}$  is almost constant in the case of ITO–Al electrode, whereas the value of  $V_{oc}$  decreases first and becomes constant by using polished mylar surface as electrode. In this context, the real reason for the decreasing value of  $V_{oc}$  is not known.

## Conclusion

In this work, the photovoltaic properties of crystal-violet-dye-sensitised solid-state PEC have been described. The films were prepared by spin coating technique. The crystal-violet-based PEC shows photovoltaic property, but the power conversion efficiency is quite poor of the order of 0.144%. Aluminium- and indium tin oxide (ITO)-coated glass plates are used as counter electrodes in our previous experiment where the value of power conversion efficiency was low. In this present work, the back electrode (Al) is replaced by a polished Al-coated mylar to enhance the power conversion efficiency up to 0.670%. It is expected that the work function of aluminium and polished Al-coated mylar is the same. The difference in power conversion efficiency mainly depends on confinement of optical energy within two electrodes which is enhanced because of multiple reflection in the presence of reflecting mylar layer. Our investigation shows that the method of optical confinement through internal reflection from Al-coated mylar surface increases the value of photovoltaic parameters.

**Acknowledgements** The authors thank Prof. A. N. Basu, Department of Physics and Prof. S. C. Bera, Department of Chemistry, Jadavpur University, Kolkata-32 for their valuable discussions. The

authors are also thankful to the Defence Research Development Organisation of India for funding the project on the development of organic photovoltaic devices.

## References

1. Al-Mohamad A (2004) *Energy Convers Manag* 45:2661–2665
2. Roman LS, Mammo W, Andersson MR, Inngan O (1997) *Adv Mater* 9:1164
3. Bandara LRAK, Dasanayake MAKL, Ekanayake GVK, Eleperuma OA, Wearaman TTK (2000) *Solid State Ion: Sci and Tech* 493
4. Barbec CJ, Sariciftci N Serdar (1999) *Semiconducting polymers*. In: Hadziioannou G, Hutten PFV (ed). Wiley-VCH, New York, Ch 15
5. Gebeyehu D, Brabec CJ, Sacriciftci NS (2002) *Thin Solid Films* 403–404:271–274
6. Kim H-S, Ha CS, Lee J-K (2001) *Synth Met* 117:289–291
7. Petritsch K (2000) Thesis, Cambridge and Graz July
8. Gebeyehu D, Pfeiffer M, Maennig B, Drechsel J, Werner A, Leo K (2004) *Thin Solid Films* 451–452:29–32
9. Geens W, Poortmans J, Jain SC, Nijs J, Mertens R, Veenstra SC, Krasnikov VV, Hadziioannou G (2000) *Sol Energy Mat Sol Cells* 61:43–51
10. Birkmire RW, Eser E (1997) *Annu Rev Mater Sci* 27:625
11. Orgassa K, Schok HW, Werner JH (2003) *Thin Solid Films* 431–432:387–391
12. Brendel R, Scholten D (1999) *Appl Phys A* 69:201
13. Mizuhashi M, Cotoh Y, Adachi K (1988) Texture morphology of SnO<sub>2</sub>:F films and cell reflectance. *Jpn J Appl Phys* 27(11):2053–2061
14. Schropp REI, Zeman M (1998) *Amorphous and microcrystalline silicon solar cell*. Kluwer, Boston
15. Dey SK, Manik NB, Bhattacharya S, Basu AN (2001) *Synth Met* 118:19
16. Dey SK, Manik NB (2001) *Appl Biochem Biotechnol* 96:55
17. Haldar A (2005) *Indian J Phys Pharmacol* 79:765
18. Haldar A (2005) *Ionics* 11:315
19. Haldar A, Maity S, Manik NB (2007) *Ionics* 153
20. Bhattacharya AJ, Banerjee S, Middya TR, Tarafdar S (1998) *Fractals* 6:285
21. Funahashi M, Hanna J-I (1999) *Appl Phys Lett* 74:2584
22. Campbell IH, Smith DL, Neef CJ, Ferraris JP (1998) *Appl Phys Lett* 72:2565
23. deMello JC, Tessler N, Graham SC, Friend RH (1998) *Phys Rev B* 57:12951
24. Smith DL (1997) *J Appl Phys* 81:2869
25. Cao Y, Pei Q, Andersson MR, Yu G, Heeger AJ (1997) *J Electrochem Soc* 114:L317
26. Yang J, Shen J (1999) *J Appl Phys* 85:2699